UPGRADED ECE RADIOMETER ON THE TORE SUPRA TOKAMAK

J.L Ségui [1], D. Molina [1], M.Goniche [1] , G. Y. Antar [2] , P. Maget [1], V.S. Udintsev [1], A. Krämer-Flecken[3]

[1] DRFC, CEA-Cadarache, Association CEA-Euratom, 13108 Saint-Paul-lez-Durance, France
[2] Center for Energy Research, UCSD, 9500 Gilman Dr., La Jolla CA 92093, USA
[3]IPP Forschungszentrum Jülich GmbH, D-52425, Jülich, Germany

e-mail: segui@drfc.cad.cea.fr

Abstract

An upgraded 32-channel heterodyne radiometer, 1GHz spaced, is used on the Tore-Supra tokamak to measure the electron cyclotron emission (ECE) in the frequency range 78-110 GHz for the ordinary mode (O: $E \parallel B, k \perp B$) and 94-126.5 GHz for the extraordinary mode (X: $E \perp B$, $k \perp B$). From now radial resolution is essentially limited by ECE relativistic effects related to electron temperature and density, not by the channels frequency spacing. For example, this leads to precise electron temperature mapping during magneto hydrodynamic activities (MHD).

In the equatorial plane, we use a dual polarisation Gaussian optics lens antenna. It has low spreading and a perpendicular line-of-sight ($k \perp B$) that gives ECE measurements very low refraction and Doppler effects. Assuming that the plasma is a black body and there is no overlap between ECE harmonics, one can deduce the electron temperature profile by using the first harmonic ordinary mode (O1) or the second harmonic extraordinary mode (X2). The principle radio frequency emitter (RF) has its frequencies down shifted into intermediary frequencies (IF) that span from 2 to 18 GHz in the single side band mode (SSB). It is amplified by low noise IF amplifiers before forming channels.

A separate O/X mode RF front-end allows the use of an IF electronic mode selector. This gives the potentiality of simultaneous O/X mode measurements in the 94-110 GHz.

RF and IF filters reject the gyrotron frequency (118 GHz) in order to perform electron temperature measurements during electron cyclotron resonance heated plasmas.

A precise absolute spectral calibration is performed outside the tokamak vacuum vessel by using a 600°C black body hot source, a double coherent digital signal averaging (trigger, turn and clock) on the waveform generated by a mechanical chopper, and a simulated tokamak window. The use of differential electronics and strong electromagnetic shielding improves also the calibration precision.

The fast and slow data acquisition systems are free of aliasing effects.

All these precautions lead to ECE temperature profiles which are very consistent with Thomson scattering measurements (absolute precision +/-6%, relative precision between channels +/-3%). This relative precision is improved by doing same ohmic plasmas with small changes in the magnetic field.

Using analytical formulas, post-pulse data processing takes routinely into account the total magnetic field and the Maxwellian relativistic radial shift to improve radial location estimate.

These formulates are compatible with real time processing in order to control the plasma.

We are preparing temperature fluctuation measurements by using two tuning IF YIG filters, the principle and the set-up will be described in the paper. The goal is to achieve two channels having 100 MHz bandwidth and tuneable central frequencies in order to do cross-correlation measurements.

1) INTRODUCTION

The Tore-Supra heterodyne radiometer [1] has been recently upgraded. It can be used to measure the electron cyclotron emission in the frequency range 78-110 GHz at the first harmonic ordinary mode (O_1) or 94 –126.5 GHz at the second harmonic extraordinary mode (X_2) by using 32 channels (1 GHz spaced, 500 MHz bandwidth).

2) DIAGNOSTIC DESCRIPTION

The schematic of the new heterodyne radiometer is shown in figure 1.

In the tokamak equatorial plane , a dual polarisation Gaussian optics lens antenna with a perpendicular line of sight (with respect to the magnetic field) and a low spreading beam (full width half maximun power = 1.47 degree) gives ECE measurements with very low Doppler ($k_{//}$=0) and refraction effects . A precise RF waveguide attenuator is used to complete the linearity range between calibration and plasmas.

The principle is RF down shifted frequencies into IF intermediary frequencies (2 to 18 GHz) in the single side band mode (SSB) . This last one is obtained by means of high pass millimetric RF filter (image rejection) and low noise , low loss conversion balanced mixers driven by Gunn local oscillators (LO). The IF frequencies are given by the following equation:

$$f_{IF} = |nf_{RF} \pm mf_{LO}|$$

We put a low pass filter to overcome IF frequencies due to higher LO harmonics with respect to the above equation (only on the O mode RF front end because ECE harmonics spectrum decrease rapidly as n increase) .

RF high-pass filter skirt selectivity (10 to 12 db/GHz below the cutoff frequency, i.e LO rejection>20 db), RF isolator isolation (>27 db), good LO/RF mixer isolation (>20 db), good coupler directivity (>27 db), and IF filter selectivity prevent any LO power or noise mixer power to disturb calibration by a 600°C black body (P_{BB} =-94.4 dbm where P_{BB} = kT B_{IF},T=600 °C, B_{IF} = 500 MHz, k=1.6 10^{-23}).

As the radiometer is near the tokamak , wide-band RF ferrite isolators have a double magnetic shielding with mumetal and iron (like Russian dolls).

Lowpass RF and bandpass IF filters reject the gyrotron frequency (118 GHz) in order to perform temperature measurements during Electron Cyclotron Resonance Heating plasmas.

Low noise 2-18 GHz IF amplifiers (30 db gain, noise figure 3 db max) allow to get enough IF power with a good signal to noise ratio.

Separated O/X mode RF front-end allow the use

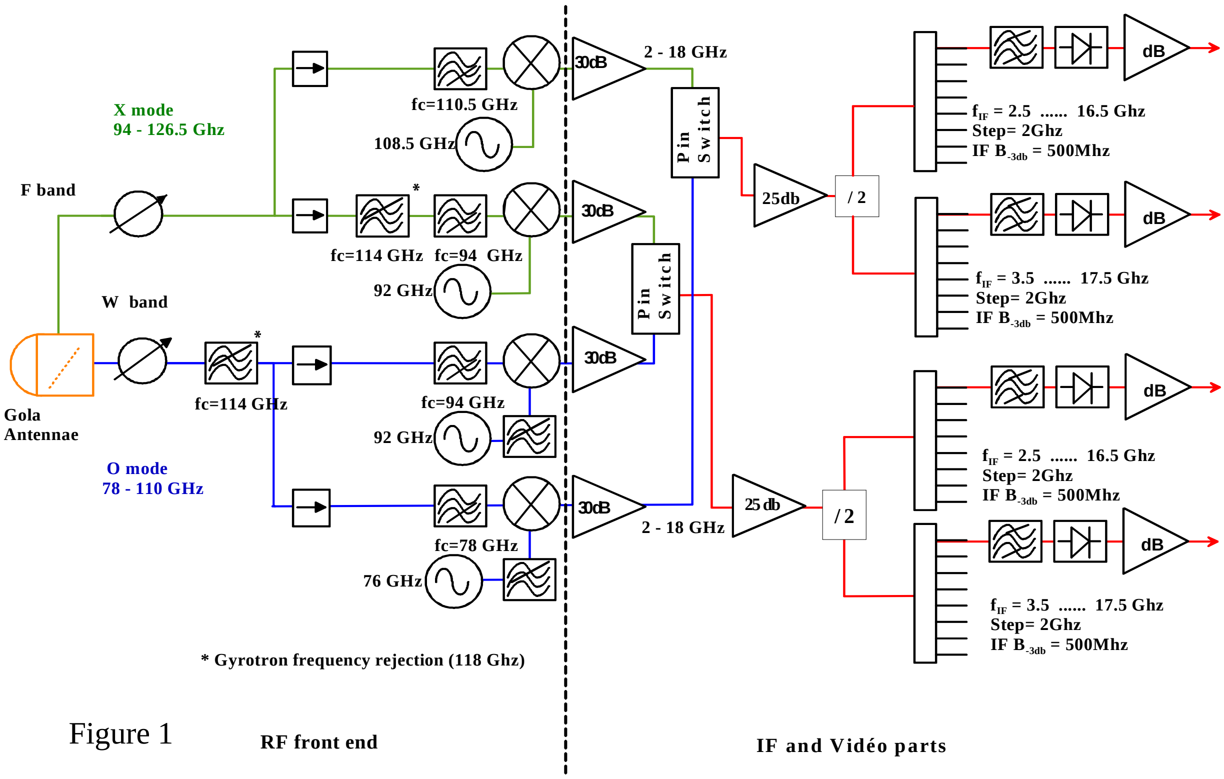

Figure 1

of IF electronic mode selectors (PIN switch). These last one give the potentiality of simultaneous O/X mode measurements in the 94 -110 GHz RF band for ECE studies.

2-18 GHz IF power amplifiers (25 db gain, 25 dbm at 1db compression point) allow higher dynamic range.

After power splitting, every channel is done by using selective IF pass-band filter (B_{IF}=500 MHz) and a video detection with a low noise and high linearity range schottky diode detector (tangential sensitivity= -52 dbm min for a video bandwidth B_V= 1MHz and a noise figure N_F=2 db and linear range ,versus input power, up to –15dbm).

Finally low noise video amplifiers, with low-pass filters (bandwidth B_{V0}=100 kHz) and differential drivers, give signals to isolated differential electronics data acquistion systems , located 50 meters farther, and which can act simultaneously in two modes:

-slow acquisition mode during all the plasma duration: 32 channels 1 ms sampling without aliasing (bandwith B_{V1}=400 Hz)

-fast acquisition mode during time plasma windows triggered by plasma phenomenon: 32 channels 10 µs sampling without aliasing (bandwith B_{V2}=40 kHz)

The tokamak toroidal coil current acts pin Switch mode selectors and the frequencies channels are the following:

Itor >730A : O-mode

Step 1 GHz: 32 channels

$f1_{GHz}$=[78.5 to 93.5]; $f2_{GHz}$=[94.5 to 109.5];

Itor < 730A : X-mode

Step 1 Ghz: 32 channels

$f1_{GHz}$=[111 to 126]; $f2_{GHz}$=[94.5 to 109.5];

A precise absolute out-side tokamak vessel calibration is performed by using:

- an hot black body (600°C) and a rotating chopper
-a diagnostic set-up which can be moved without changing the instrumental function
- a local platinum temperature probe to correct sensitivity drifts (–2.7% / °C) ,
- a simulation of the tokamak window, which has no Fabry-Pérot effects
- efficient coherent addition techniques.

To perform these last one the data acquisition system use a trigger and a clock synchronous to the chopper rotation. In this way the black body modulating signal bb(t) is decorrelated from Gaussian noise N(t) , which is limited to the 0.3-300Hz band by a video bandpass filter. Differential electronics are used to minimise electromagnetics radiations pollution ac(t) due to AC supplies. After coherent addition we can obtain a good estimate of bb(t):

$$V_i(t) = bb(t) + N(t) + ac(t)$$

where $V_i(t)$ is one of the detector voltages

The intercalibration precision between channels is also improved by using same ohmic plasmas having solely small changes on the magnetic field .

3) ROUTINE DATA PROCESSING & EXPERIMENTAL RESULTS

3.1) ECE basis ($k_{//}$=0 , low Larmor radius approximations, no harmonic overlaping)

In the following parts, after some ECE basis recalls, we will discribe successively:

- radial shift due to a relativistic maxwellian distribution function (numeric and analytical formulations)
- radial corrections when taking into account the total magnetic field (analytical formulation).
- the strong refraction detection

We can find below the relativistic ECE resonance condition (γ relativistic factor), the measured radiative temperature T_{rad} related to the radiative intensity I_ω, the Kirchoff law which links the ECE emissivity β_ω to the ECE absorption α_ω , the radiative intensity taking into account the effective wall reflexion coefficient ρ_{eff} , the optical depth τ_ω, the intensity absorption coefficient in the O mode (n=1) and the X mode (n=2).

$$\omega = \frac{n\omega_{ce}(R)}{\gamma} \quad T_{rad} = \frac{8\pi^3 c^2}{\omega^2} I_\omega \quad \frac{\beta_\omega}{\alpha_\omega} = \frac{\omega^2}{8\pi^3 c^2} kT_e$$

$$I_\omega = \frac{\int_{R0-a}^{R0+a} \beta_\omega(\ell) e^{-\tau_\omega(l)} dl}{1-\rho_{eff} e^{-\tau_\omega}} \qquad \tau_\omega(\ell) = \int_\ell^{R_0+a} \alpha_\omega(\ell') d\ell'$$

$$\alpha_{o\omega} = \frac{4\sqrt{\pi}}{15}\frac{\omega}{c} N_o \left(\frac{\omega_{pe}}{\omega_{ce}}\right)^2 \mu \left(\frac{\omega_{ce}}{\omega} - 1\right)^{\frac{5}{2}} \exp\left(-\mu\left(\frac{\omega_{ce}}{\omega} - 1\right)\right)$$

$$\alpha_{x\omega} = \frac{4\sqrt{\pi}}{15}\frac{\omega}{c} N_x \left(\frac{\omega_{pe}}{\omega_{ce}}\right)^2 \mu \left(\frac{2\omega_{ce}}{\omega} - 1\right)^{\frac{5}{2}} \exp\left(-\mu\left(\frac{2\omega_{ce}}{\omega} - 1\right)\right)$$

Where $\mu = \frac{m_e c^2}{T_e}$, N_O and N_X are the refraction index for the O mode and the X mode.

3.2) ROUTINE DATA PROCESSING

a) Maxwellian relativistic shift

The relativistic shift δR can be approached by an analytic formulation [2,3]:

$$\delta R = R \frac{T_e}{511} \left(\frac{511}{T_e R} \frac{75 \; c\,\omega_{ce}^2}{8\sqrt{\pi}\,\omega\omega_{pe}^2 N_r} \right)^{\frac{2}{7}}$$

where $\omega = n\omega_{ce}$, n=1, $N_r=N_o$ or n=2, $N_r=N_x$

The good agreement between numerical and analytical simulations is given in the Omode , for example, by the figure 2 (full line : analytical , cross bar : numerical , with T_{e0}=10 keV, n_{e0}=2 10^{19}m^{-3}, cf [2]).

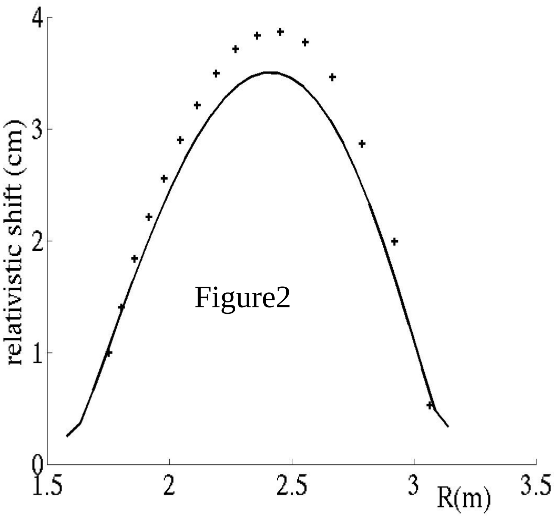

b) Total magnetic field calculations

These calculations are based on a magnetic equilibrium including Shafranov shift and magnetic ripple (B_{rip}), poloidal (B_{pol}), diamagnetic (B_{dia}) and paramagnetic (B_{para}) fields corrections to the vacuum toroidal field (B_{vac}). We assume a density current profile of the form $J_0(1 - \rho^2)^{\nu_j}$, where ρ is the normalized radial coordinate and J_0,ν_j are obtained by magnetic measurements with the following formula [4]:

$$J_0 = \frac{I_p}{\pi a^2}(1+\nu_j), \nu_j = \frac{1}{0.89}(e^{li} - 1.65)$$

where I_p is the plasma current, li the internal plasma inductance.

The expressions used for the different components of the total magnetic field B_{tot} are:

$$B_{tot} = \sqrt{(B_{vac} - B_{rip} + B_{para} + B_{dia})^2 + B_{pol}^2},$$

assuming a radial component B_r=0,

where: $B_{vac} = B_{0vac} \frac{R_{0vac}}{R}$,

$$B_{pol} = -\frac{\mu_0 a J_0}{2(\nu_J + 1)\rho}\left[\left(1-\rho^2\right)^{\nu_J + 1} - 1\right],$$

$$B_{dia} = -2\mu_0 \frac{n_e T_e}{B_0},$$

$$B_{para} = \frac{\mu_0^2 a^2 J_0^2}{2(\nu_J + 1)B_0} \int_1^\rho \left[(1-\rho'^2)^{2\nu_j+1} - (1-\rho'^2)^{\nu_j}\right]\frac{d\rho'}{\rho'}$$

with an integer ν_j

$$B_{rip} = c.B_{vac}\exp(13.6u + 11.83u^2).\cos(N_b.phi) \quad (a)$$

with:

$$u^2 = 1 + 0.52(R - 2.04) - \sqrt{1 + 1.04(R - 2.04) - 0.27z^2}$$

$$Nb = 18; phi = 3.5°; z = 0, c = 2.2\,10^{-4}$$

where R is the radial coordinate (in m), R_{0vac}=2.36 m is the major radius of the vacuum vessel, B_{0vac} is the vacuum magnetic field at $R=R_{0vac}$, and Eq.(a) is a fit of the specific Tore Supra ripple configuration , Nb the number of coils. Plots of B_{vac} and B_{tot} versus the horizontal coordinate R for typical Tore Supra parameters are shown in Figure 3 (full line: B_{vac} , dashed line: B_{tot}).

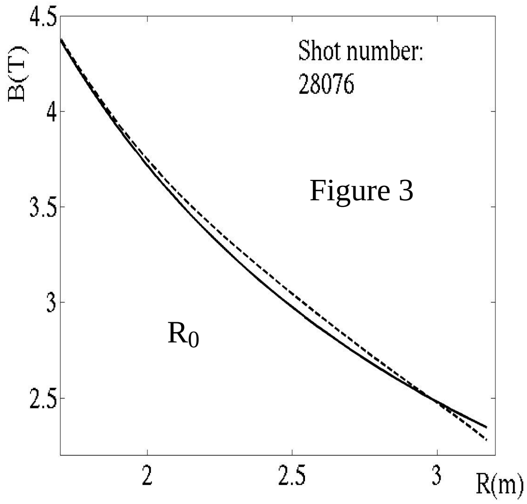

c) Strong refraction detection

-For each channel **i** we detect if there is strong refraction by doing the following test :

$\mathbf{f_i < 1.2 * f_{cut\text{-}off}(R_i)}$)

n=2

$$f^{(E)}_{cut-off} = \frac{1}{2} f_{ce} \left[1 + \left(1 + \left(\frac{2 f_{pe}}{f_{ce}} \right)^2 \right)^{\frac{1}{2}} \right] = 2 \cdot f_{ce}$$

n=1 $f^{(O)}_{cut-off} = f_{pe} = f_{ce}$

n used harmonic, with $f_{ce} = 28.B$

One has respectively :

$$f_{pe} = \sqrt{2} \cdot f_{ce} \Rightarrow n^{(E)}_{cut-off} = 1.94 \cdot 10^{19} \cdot B^2$$

$$f_{pe} = f_{ce} \Rightarrow n^{(O)}_{cut-off} = 9.72 \cdot 10^{18} \cdot B^2$$

with ne in m^{-3}, B in Tesla.

3.3) EXPERIMENTAL RESULTS

a) Calibration precision

The good calibration precision leads to ECE temperature profiles which are very consistent with Thomson scattering measurements. One can see figure 4 electron temperature profiles, versus normalized radius, given by the 32 channel heterodyne ECE radiometer and Thomson scattering diagnostics .

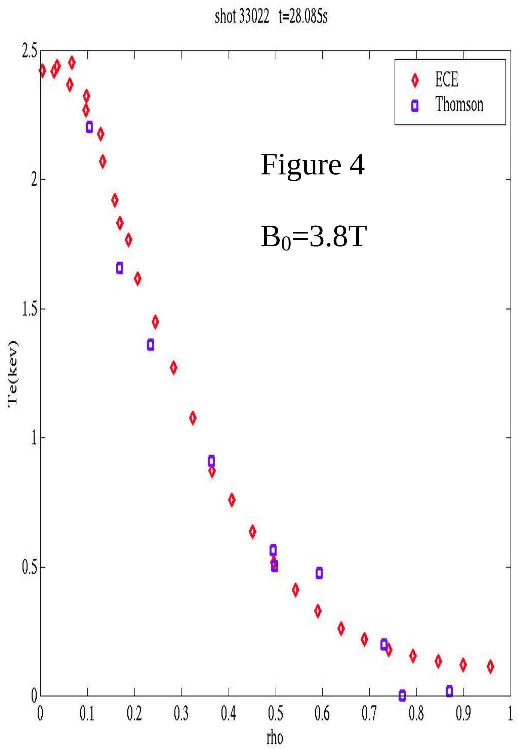

Figure 4

b) MHD measurements

Figures 5 and 6 show sawtheeth crashes measured in the slow (1ms) and the fast acquisition modes (10 µs) for two different shots. One can observe a strong (m=1, n=1) precursor for the first one and its manifestation as the hot core expulsion for the second one. In the latter case, no additional hot core presents on the former magnetic axis after 12.0965 s.

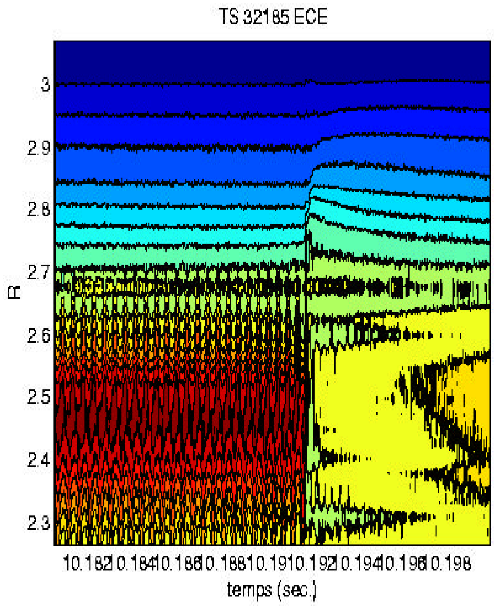

Figure 5

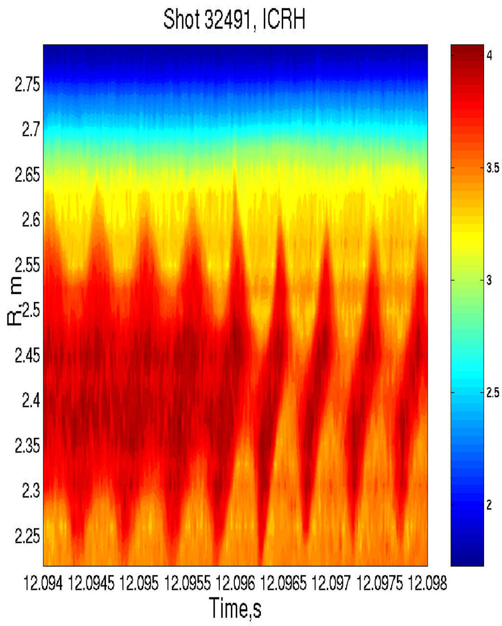

Figure 6

4) Te fluctuations measurements

4.1) Theoretical principles

The optical thick ECE $S(t)$, as measured by each radiometer channel, consists of an average $\langle S \rangle$ and a fluctuation $s(t)$ part that are proportional to the average plasma temperature $\langle T_e \rangle$, and to its fluctuating component $t_e(t)$ plus the statistical radiation noise $n(t)$.

$$S(t) = \langle S \rangle + s(t) \propto \langle T_e \rangle + t_e(t) + n(t)$$

The limits of electron temperature fluctuations measurements due to $n(t)$ is [5,6]:

$\frac{s_{RMS}}{\langle S \rangle} = \sqrt{\frac{2B_{IF}}{B_v}}$, where s_{RMS} is the root mean square amplitude of the signal fluctuation .

To measure the average amplitude of temperature fluctuations in tokamak plasmas of smaller than 1-2% one needs to get rid of the thermal noise $n(t)$.

4.2) Experimental set-up

Using a single line of sight this can be achieve by cross correlation of two ECE channel signals whose temperature fluctuations are correlated while the noise fluctuations are uncorrelated. So we propose to add the following set-up (dashed line: cf figure 7) to the existing radiometer, following the [7] techniques. The goal is to achieve two channels having 100 MHz bandwidth and tuneable central frequencies to shift the plasma sample volume in the radial space.

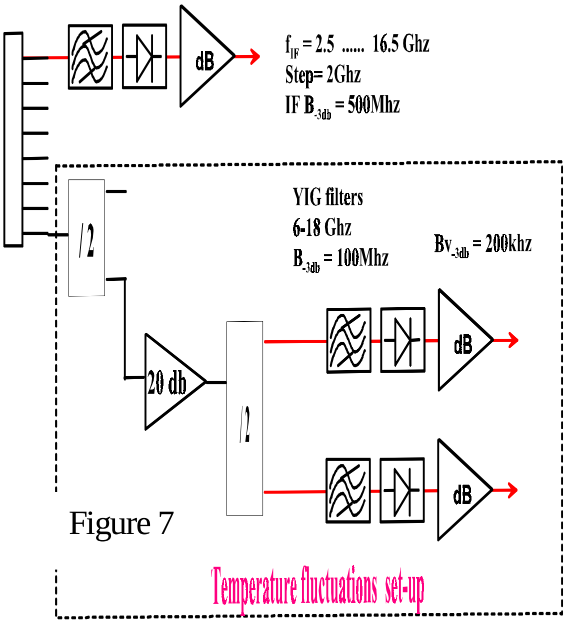

Figure 7

The statistical noise level can be defined as follows [8,9]:

$$\Delta\left(\frac{t_{eRMS}}{\langle T_e \rangle}\right) = \sqrt{\frac{\Delta r_{12}}{\langle S_1 \rangle \langle S_2 \rangle}} = M^{-\frac{1}{4}} \sqrt{\frac{\sigma_1}{\langle S_1 \rangle} \frac{\sigma_2}{\langle S_2 \rangle}}$$

where r_{12} is the cross correlation fonction at zero time delay, σ_1 and σ_2 are the standard deviations of s_1 and s_2, M is the total number of samples.

The video bandwidth is 200 kHz and acquisition will be done without aliasing effects.

M will be of several 10^6 samples to get out efficiently the thermal noise $n(t)$.

5) CONCLUSION

The Tore-Supra ECE radiometer has reached a good degree of maturity. A good absolute calibration is performed and radial resolution is only due to relativistic effects (32 channels). Routine ECE data processing takes into account radial relativistic shift and the total magnetic field using analytic formulations which can be applied in real time processing to perform plasma control. Temperature fluctuation measurements will be done soon.

References

[1] J.L Ségui et al ,169 (1997), EC 10 proceedings, Ameland, the Netherlands, 1997

[2] J.L Ségui et al , 209 (2002), EC12 proceedings, Aix en Provence, 2002

[3] I.Fidone *et al* , Phys.Plasmas 3(6) 2331, June 1996

[4] Tokamaks by John Wesson , p114 & 120, 2rd edition, Clarendon Press, Oxford, 1997

[5] S.Sattler,HJ.Hartfuss,Plasmas Phys. Control. Fusion **35**,1285 (1993)

[6] H.J Hartfuss,M.Hase,p119 EC10 proceedings Ameland April 6-11,1997

[7] C.L Rettig, *et al*, Rev.Sci.Instrum. 68(1), January 1997

[8] G.Cima *et al*, Phys.Plasmas **2**,720 (1995)

[9] M.Hase H.J Hartfuss,p131 EC10 proceedings Ameland April 6-11,1997